EURASIP Journal on Wireless Communications and Networking 2005:4, 554–564

Throughput Analysis of Fading Sensor Networks with Regular and Random Topologies

Xiaowen Liu
Department of Electrical Engineering, University of Notre Dame, Notre Dame, IN 46556, USA
Email: xliu4@nd.edu

Martin Haenggi
Department of Electrical Engineering, University of Notre Dame, Notre Dame, IN 46556, USA
Email: mhaenggi@nd.edu

Received 30 November 2004; Revised 5 June 2005

We present closed-form expressions of the average link throughput for sensor networks with a slotted ALOHA MAC protocol in Rayleigh fading channels. We compare networks with three regular topologies in terms of throughput, transmit efficiency, and transport capacity. In particular, for square lattice networks, we present a sensitivity analysis of the maximum throughput and the optimum transmit probability with respect to the signal-to-interference ratio threshold. For random networks with nodes distributed according to a two-dimensional Poisson point process, the average throughput is analytically characterized and numerically evaluated. It turns out that although regular networks have an only slightly higher average link throughput than random networks for the same link distance, regular topologies have a significant benefit when the end-to-end throughput in multihop connections is considered.

Keywords and phrases: throughput, Rayleigh fading, slotted ALOHA, network topology, interference.

1. INTRODUCTION

A sensor network [1] consists of a large number of sensor nodes which are placed inside or near a phenomenon. Uniformly random or Poisson distributions are widely accepted models for the location of the nodes in wireless sensor networks, if nodes are deployed in large quantities and there is little control over where they are dropped. A typical scenario is a deployment from an airplane for battlefield monitoring. On the other hand, depending on the application, it may also be possible to place sensors in a regular topology, for example, in a square grid.

Throughput is a traditional measure of how much traffic can be delivered by the network [2, 3]. There is a rich literature on throughput capacity for wireless networks [2, 4, 5] with random or regular topologies. The seminal paper [2] shows that, for peer-to-peer traffic, in a static two-dimensional network with N nodes and $N/2$ randomly selected source-destination pairs, the end-to-end throughput of a connection is $\Theta(W/\sqrt{N})$, where W is the maximum transmission rate for each node. The reason for this poor scaling behavior is that the *per-link*[1] throughput remains constant while the number of hops grows with $\sqrt{N}$. Marco et al. [6] show that with many-to-one traffic, the per-node transport capacity is $\Theta(1/N)$. Such "order of" results do not provide any guidelines for protocol design, since the scaling behavior is very robust against changes in MAC and routing protocols [7]. All the above research work assumes networks with randomly located nodes. There are also research efforts focusing on networks with regular topologies. Silvester and Kleinrock [4] calculate the throughput of regular square networks with a slotted ALOHA channel access scheme. Xie and Kumar [7] prove that the $\Theta(N)$ upper bound on transport capacity is tight for regular networks where nodes are placed on integer lattice points for path loss exponents greater than 3 and is achieved by multihop transmission. De et al. [8] compare the performance of regular topologies with random topology in wireless CDMA sensor networks. The authors in [9, 10] evaluate the performance for regular grid and random topologies. They assume a "torus" network to avoid boundary effects and use the expected interference power to replace the exact interference power. In particular at high load,

[1] The link throughput is the total achievable throughput over a link, aggregated over the flows or connections that are served by the link.

replacing the actual interference by its mean yields overly pessimistic results. Indeed, the expected interference may be infinite [11].

Most of the work above is based on a "disk model," where it is assumed that the radius for a successful transmission of a packet has a fixed and deterministic value, irrespective of the condition and the realization of the wireless channel. Such simplified link models ignore the stochastic nature of the wireless channel. Our analysis is based on a Rayleigh fading channel model, which includes both large-scale path loss and stochastic small-scale variations in the channel characteristics. Note that even with static nodes as assumed in this paper, the channel quality varies because any movement in the environment affects the multipath geometry of the RF signal, which is easily confirmed experimentally [12, page 45]. The significant variation of the link quality when nodes are immobile is also pointed out in [13, 14, 15], and the shortcomings of the "disk model" are discussed in [11].

This paper addresses the throughput problem for large sensor networks with Rayleigh fading channels. To provide insight on the impact of the topology on the network performance, we compare networks with a random topology and three regular topologies. Placing nodes in regular lattices has an obvious advantage in terms of coverage [16], so we are not addressing coverage issues here. We define the (per-link) throughput as the expected number of successful packet transmissions of a given link per timeslot. The *end-to-end* throughput over a multihop connection, defined as the minimum of the throughput values of the links involved, is a performance measure of a route and the MAC scheme.

We consider a variant of the slotted ALOHA channel access scheme, originally devised in [17], that takes advantage of spatial reuse. It is assumed, as in [4, 18, 19, 20], that in every timeslot, each node transmits independently with a certain fixed probability p. While often a "heavy traffic" model is used [4, 20], where nodes always have packets to transmit and p only reflects the channel access probability, we do not restrict ourselves to this "MAC-centric" case. Rather, we consider p to be composed of two factors, that is, $p = p_q p_t$, where p_q is the probability that there is a packet in a node's queue awaiting transmission, and p_t is the probability of transmission conditioned on having a packet in the queue (the channel access probability). So, p_q is given by the traffic model, p_t is the actual slotted ALOHA channel access probability, and p is the unconditioned probability of transmission. The heavy traffic case mentioned above corresponds to $p_q = 1$, $p_t = p$, and the other extreme case is $p_q = p$, $p_t = 1$, where Bernoulli traffic is generated with probability p_q and each node with a packet to transmit has immediate access to the channel. Since there is no need for a MAC scheme in this case, we may denote it as "traffic-centric." Hence, the decomposition of p shows that the throughput analysis and optimization with respect to p in fact includes a range of traffic intensities and channel access probabilities. The Bernoulli traffic model is well justified by the following three observations: (1) in [18], it was shown that the traffic from a slotted ALOHA population of nodes can indeed be modeled as Bernoulli; (2) in [21, page 278], it is pointed out that the retransmission traffic is usually Bernoulli (since an unsuccessfully transmitted packet reenters the queue); and (3) the Bernoulli traffic model is memoryless and thus the discrete-time counterpart of the ubiquitous Poisson model.

The traffic distribution in a sensor networks is usually spatially and temporally bursty, that is, busy periods alternate temporally and busy areas alternate spatially with periods and areas with little or no traffic. It may therefore be impractical to employ reservation-based MAC schemes such as TDMA and FDMA that require a substantial amount of coordination traffic and cannot be implemented efficiently and in a fully distributed fashion.[2] In any case, the slotted ALOHA scheme is the simplest meaningful MAC scheme and therefore provides a lower bound on the performance for more elaborate schemes. Since areas of the network or periods with little or no traffic pose no problems, our analysis focuses on and applies to busy areas and busy periods of the network where collisions are unavoidable and the throughput is interference-limited. During such a burst of traffic, we assume that the parameters p, p_q, and p_t remain constant. An important example of a busy area is certainly the critical area around the base station or fusion center, where traffic accumulation due to the many-to-one transmission scheme often results in heavy traffic [22].

In Section 2, the Rayleigh fading link model is introduced. For a slotted ALOHA MAC scheme, the conditional success probability of a transmission for a node given the transmitter-receiver and interference-receiver distances is derived. Section 3 evaluates the throughput for regular networks with three topologies and compares their performance. Section 4 investigates the average throughput for random networks for fixed and random transmitter-receiver distances d_0. This section also analyzes the transport capacity and end-to-end throughput. Section 5 concludes the paper.

2. THE RAYLEIGH FADING LINK MODEL

We assume a narrowband Rayleigh block fading channel. A transmission from node i to node j is successful if the signal-to-noise-and-interference ratio (SINR) γ_{ij} is above a certain threshold Θ that is determined by the communication hardware and the modulation and coding scheme [14]. The SINR γ is given by $\gamma = Q/(N_0 + I)$, where Q is the received power, which is exponentially distributed with mean $\bar{Q}$. Over a transmission of distance d with an attenuation d^{α}, we have $\bar{Q} = P_0 d^{-\alpha}$, where P_0 denotes the transmit power, α is the path loss exponent. N_0 denotes the noise power, and I is the interference power, that is, the sum of the received power from all the undesired transmitters. Our analysis is based on the following theorem.

Theorem 1. *In a Rayleigh fading network with slotted ALOHA, where nodes transmit at equal power levels with probability p, the success probability of a transmission given a desired transmitter-receiver distance d_0 and n other nodes at*

[2] In general, this problem is NP-hard.

distances d_i ($i = 1, \ldots, n$) is

$$P_{s|d_0,\ldots,d_n} = \exp\left(-\frac{\Theta N_0}{P_0 d_0^{-\alpha}}\right) \cdot \prod_{i=1}^{n}\left(1 - \frac{\Theta p}{(d_i/d_0)^{\alpha} + \Theta}\right), \quad (1)$$

where P_0 is the transmit power, N_0 the noise power, and Θ the SINR threshold.

Proof. Let Q_0 denote the received power from the desired transmitter and Q_i, $i = 1, \ldots, n$, the received power from n potential interferers. All the received powers are exponentially distributed, that is, $p_{Q_i}(q_i) = 1/\bar{Q}_i e^{\cdot -q_i/\bar{Q}_i}$, where $\bar{Q}_i$ denotes the average received power $\bar{Q}_i = P_i d_i^{-\alpha}$. The cumulated interference power at the receiver is

$$I = \sum_{i=1}^{n} S_i Q_i, \quad (2)$$

where S_i is a sequence of i.i.d. Bernoulli random variables with $\mathbb{P}(S_i = 1) = p$ and $\mathbb{P}(S_i = 0) = 1 - p$. The success probability of a transmission is[3]

$$\begin{aligned}
P_{s|d_0,d_1,\ldots,d_n} &= \mathbb{E}_I\left[\mathbb{P}\left[Q_0 \geqslant \Theta(I + N_0) \mid I\right]\right] \\
&= \mathbb{E}_{Q,S}\left[\exp\left(-\frac{\Theta(\sum_{i=1}^{n} S_i Q_i + N_0)}{\bar{Q}_0}\right)\right] \\
&= \exp\left(-\frac{\Theta N_0}{\bar{Q}_0}\right)\mathbb{E}_{Q,S}\left[\prod_{i=1}^{n}\exp\left(-\frac{\Theta(S_i Q_i)}{\bar{Q}_0}\right)\right] \\
&= \exp\left(-\frac{\Theta N_0}{P_0 d_0^{-\alpha}}\right) \\
&\quad \times \prod_{i=1}^{n}\left\{P(S_i = 1) \cdot \int_0^{\infty}\exp\left(-\frac{\Theta q_i}{\bar{Q}_0}\right)\right. \\
&\qquad \left. \times\, p_{Q_i}(q_i)\,dq_i + P(S_i = 0)\right\} \\
&= \exp\left(-\frac{\Theta N_0}{P_0 d_0^{-\alpha}}\right)\prod_{i=1}^{n}\left(\frac{p}{1 + \Theta(d_0/d_i)^{\alpha}} + 1 - p\right) \\
&= \exp\left(-\frac{\Theta N_0}{P_0 d_0^{-\alpha}}\right)\prod_{i=1}^{n}\left(1 - \frac{\Theta p}{(d_i/d_0)^{\alpha} + \Theta}\right).
\end{aligned} \quad (3)$$

□

Since the throughput in large sensor networks is limited by the interference, in the following, we focus on the interference part (the second factor of (3), assuming $N_0 = 0$) to determine bounds that are fundamental in the sense that they cannot be exceeded even if the transmit power is not constrained. The first exponential term is easily evaluated if $N_0 \neq 0$.

[3] A similar calculation has been carried out in [23] for the case where in every timeslot it is known exactly which node is transmitting. In contrast, Theorem 1 incorporates the uncertainty at the MAC level: we only assume we know the probability of a transmission, but not exactly which node is transmitting in every timeslot.

Corollary 1. *Under the same assumptions as in Theorem 1 but with $N_0 = 0$ and unit transmit power $P_i = 1$, the success probability given a desired link of normalized distance $r_0 = d_0/d_0 = 1$ and n other nodes at normalized distances $r_i = d_i/d_0$ is*

$$P_{s|r_0,r_1,\ldots,r_n} = \prod_{i=1}^{n}\left(1 - \frac{p}{1 + r_i{}^{\alpha}/\Theta}\right) = \mathcal{L}_I(\Theta), \quad (4)$$

which is the Laplace transform of the interference power I evaluated at the SIR threshold Θ.

Proof. With unit transmit power, the mean power from the ith interferer at distance r_i is $1/r_i^{\alpha}$. The Laplace transform of the exponential distribution with mean $1/\mu$ is $\mu/(\mu + s)$, thus the Laplace transform of I is [24]

$$\mathcal{L}_I(s) = \prod_{i=1}^{n}\left(\frac{p r_i^{\alpha}}{r_i^{\alpha} + s} + 1 - p\right) = \prod_{i=1}^{n}\left(1 - \frac{p}{1 + r_i^{\alpha}/s}\right). \quad (5)$$

From (3) and with $r_i = d_i/d_0$ (normalized distances), if $N_0 = 0$,

$$P_{s|r_0,r_1,\ldots,r_n} = \prod_{i=1}^{n}\left(1 - \frac{p}{1 + r_i{}^{\alpha}/\Theta}\right), \quad (6)$$

we get (4). □

3. REGULAR NETWORKS

In this section, we investigate networks with three regular topologies (square, triangle, hexagon) in which every node has the same number of nearest neighbors and the same distance to all nearest neighbors.

3.1. Square networks

We first analyze square networks with N nodes placed in the vertices of a square grid with distance 1 between all pairs of nearest nodes (density 1). The next-hop receiver of each packet is one of the four nearest-neighbor nodes of the transmitter, so the transmitter-receiver distance $d_0 = 1$. If the receiver node O is located in the center of the network as shown in Figure 1 and node A is the desired transmitter, the success probability for node O based on (6) can be written as

$$\begin{aligned}
P_s(p) &= \left(1 - \frac{\Theta p}{1^{\alpha} + \Theta}\right)^3 \cdot \left(1 - \frac{\Theta p}{(\sqrt{2})^{\alpha} + \Theta}\right)^4 \\
&\quad \times \prod_{i=2}^{\sqrt{N}/2}\left\{\left(1 - \frac{\Theta p}{i^{\alpha} + \Theta}\right)^4\right. \\
&\qquad \cdot \left(1 - \frac{\Theta p}{(\sqrt{2i^2})^{\alpha} + \Theta}\right)^4 \\
&\qquad \left. \cdot \prod_{j=1}^{i-1}\left(1 - \frac{\Theta p}{(\sqrt{i^2 + j^2})^{\alpha} + \Theta}\right)^8\right\}.
\end{aligned} \quad (7)$$

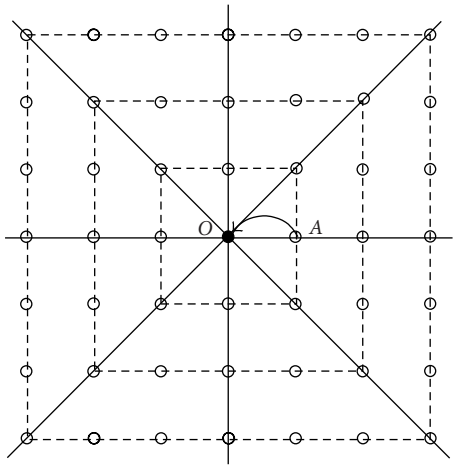

FIGURE 1: The topology of a square network. Node O is the receiver and node A is the desired transmitter such that the link distance $d_0 = |OA| = 1$.

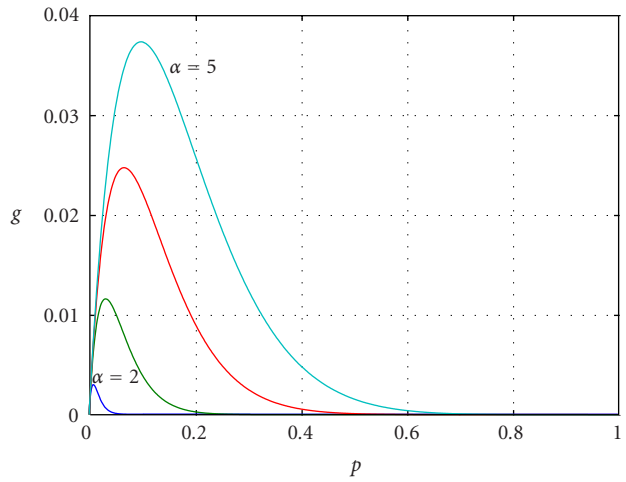

FIGURE 2: The analytic throughput $g(p)$ based on (7) for a square network with 40×40 nodes, with $\Theta = 10$.

The first term in (7) accounts for the other three nearest-neighbor nodes of the receiver; the second term for the 4 diagonal nodes at distance $\sqrt{2}$; all the other terms from the nodes located on the dashed squares with edge ≥ 2 in Figure 1. The throughput[4] is given by

$$g(p) = p(1-p)P_s(p), \tag{8}$$

where p is the probability that A transmits and $1-p$ is the probability that O does not transmit in the same timeslot. Note that g is the throughput achievable with a simple ARQ scheme (with error-free feedback) [25]. The analytic throughput $g(p)$ based on (7) and (8) for a regular square network with 40×40 nodes with node density $\lambda = 1$ is displayed in Figure 2. For $\alpha = 4$, the maximum throughput $g_{\max} = 0.0247$ is achieved at an optimal transmit probability $p_{\text{opt}} = 0.066$. The transmit efficiency, defined as $T_{\text{eff}} = g_{\max}/p_{\text{opt}}$, is 37.4%.

For the *sensitivity* analysis of the throughput with respect to Θ, we need to determine $p_{\text{opt}}(\Theta)$ and $g_{\max}(\Theta)$. We use three analytic approximations for $p_{\text{opt}}(\Theta)$ and $g_{\max}(\Theta)$. From (6), g can be written as

$$g = p(1-p)\prod_{i=1}^{n}\left(1 - \frac{p}{1 + r_i^{\alpha}/\Theta}\right), \tag{9}$$

where $r_i = d_i/d_0$.

Since $p_{\text{opt}} = \arg\max_p g(p) = \arg\max_p \log(g(p))$, we maximize

$$\log(g) = \log(p) + \log(1-p) + \sum_{i=1}^{n}\log\left(1 - \frac{p}{1 + r_i^{\alpha}/\Theta}\right), \tag{10}$$

using $\log(1+x) \approx x$ for small x,[5] yielding

$$p_{\text{opt}}^2 - p_{\text{opt}}(1+2s) + s = 0, \tag{11}$$

with

$$s = \frac{1}{\sum_{i=1}^{n}(1/(1 + r_i^{\alpha}/\Theta))}. \tag{12}$$

Note $r_i = d_i$ for $d_0 = 1$. So, p_{opt} is given by

$$p_{\text{opt}} = s + \frac{1}{2}\left(1 - \sqrt{1+4s^2}\right). \tag{13}$$

$g_{\max}$ can be obtained by $g_{\max} = p_{\text{opt}}(1 - p_{\text{opt}})P_s(p_{\text{opt}})$, where $P_s(p_{\text{opt}})$ is obtained by plugging p_{opt} into (7). This method is called *Analytic 1*.

For $\alpha = 4$, we use i^2 to approximate d_i^4 for the nodes located in one quadrant. As shown in Figure 3, the distance of node i ($i = 1, \ldots, 8$) in the first quadrant to the receiver node O is d_i. Table 1 compares d_i^4 and i^2 for $i = 1, \ldots, 8$. By Euler's summation formula, $d_i^4 \approx i^2$ allows a simplification (the node at distance 1 is the desired transmitter):

$$\sum_{i=2}^{k+1}\frac{1}{1 + i^2/\Theta} \approx \sqrt{\Theta}\left(\arctan\frac{k+3/2}{\sqrt{\Theta}} - \arctan\frac{3}{2\sqrt{\Theta}}\right). \tag{14}$$

For $k \to \infty$,

$$s \approx \frac{1}{4\sqrt{\Theta}(\pi/2 - \arctan(3/2\sqrt{\Theta}))}, \tag{15}$$

[4]The throughput is calculated as the throughput of the center link of the busy area under consideration. This is the worst case since most other nodes experience a lower interference. In the case of infinite networks, the interference distribution is the same at every node.

[5]The approximation is accurate for p in the range of interest, that is, $0 < p < 0.3$.

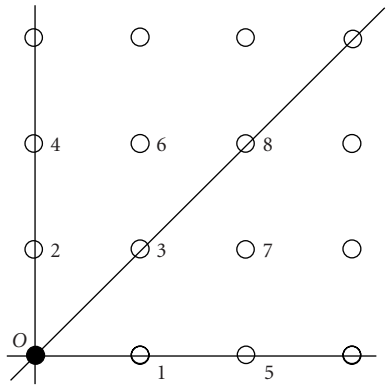

Figure 3: Node numbering scheme pertaining to Table 1 for nodes in the first quadrant of a square network. O is the receiver.

Table 1: Comparison of d_i^4 and i^2.

i	1	2	3	4	5	6	7	8
d_i^4	1	1	4	16	16	25	25	64
i^2	1	4	9	16	25	36	49	64

where the factor 4 in (15) comes from the fact that nodes are located in 4 quadrants. Plugging (15) into (13) is our method *Analytic 2*.

In method *Analytic 3*, we use the approximation $s \approx 1/(4\sqrt{\Theta})$, which is within $\mp 20\%$ for the practical range $9/(2\cot(0.8))^2 \approx 2.4 < \Theta < 9/(2\cot(1.2))^2 \approx 14.9$, and substitute it into (13), which yields

$$p_{\text{opt}} = \frac{1}{4\sqrt{\Theta}} + \frac{1}{2}\left(1 - \sqrt{1 + \frac{1}{4\Theta}}\right). \tag{16}$$

Based on (10) and (12), $g_{\max}$ is given by

$$g_{\max} = p_{\text{opt}}(1 - p_{\text{opt}})e^{-p_{\text{opt}}/s}. \tag{17}$$

The numerical result obtained by direct maximization of (7) for different Θ is compared with the results from the three analytical approximations in Figure 4. In *Analytic 2*, approximating interfering nodes at distance d_i by the larger distance $i^{1/2}$ (shown in Table 1) results in lower interference. The interference has a more significant impact on the throughput (and p_{opt}) for small Θ (see (14)). Thus for small Θ, this lower interference leads to a higher p_{opt} than for *Analytic 1*. The transmit efficiency is $T_{\text{eff}} = g_{max}/p_{\text{opt}} = (1 - p_{\text{opt}})e^{-p_{\text{opt}}/s}$, which is monotonically increasing from $\lim_{s\to 0} T_{\text{eff}} = e^{-1} \approx 0.37$ to $\lim_{s\to\infty} T_{\text{eff}} = 1/2$. The upper bound is achieved if the interference goes to zero, in which case $p_{\text{opt}} = 1/2$ and $g_{max} = 1/4$. For the lower bound, as $s \to 0$, we have $p_{\text{opt}} \to 0$ and $g_{\max} \to 0$, and T_{eff} converges to e^{-1}. Hence, s is a measure for spatial reuse. Indeed for $s \to 0$, which happens for $\alpha \to 0$[6] or $\Theta \to \infty$, the network does not permit any spatial reuse. In this case, the transmit efficiency reduces to the efficiency of conventional slotted ALOHA [17], where for a network with N nodes, $p_{\text{opt}} = 1/N$ and $T_{\text{eff}} = \lim_{N\to\infty}(1 - 1/N)^{N-1} = e^{-1}$ [4]. The fact that our limit coincides with the limit for conventional slotted ALOHA further validates our approximations.

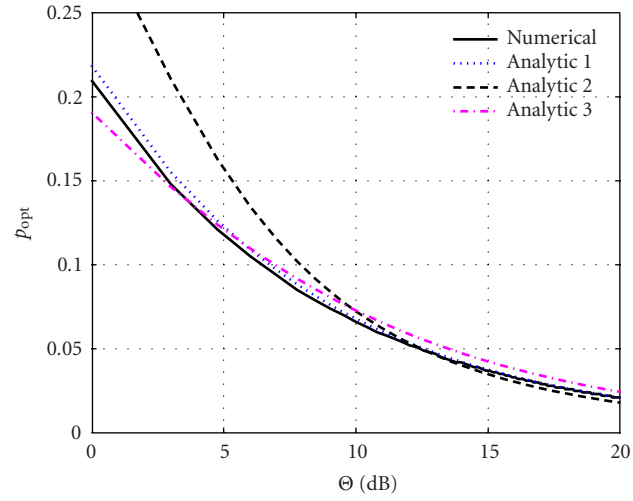

(a)

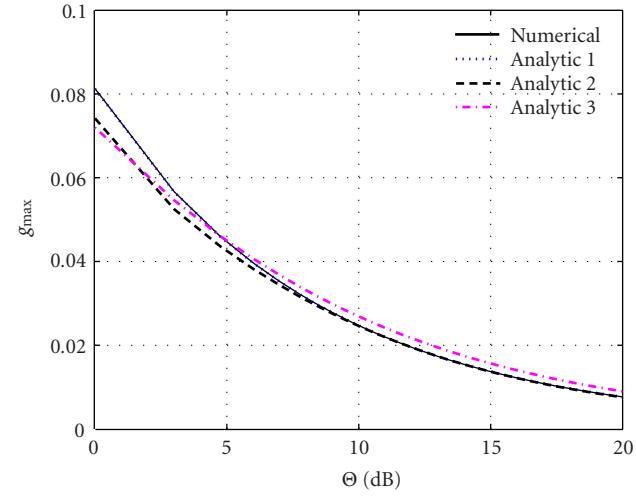

(b)

Figure 4: For a square network with 40×40 nodes and $\alpha = 4$, the numerical results and analytic results from *Analytic 1, Analytic 2*, and *Analytic 3* for (a) the relationship between p_{opt} and Θ; (b) the relationship between $g_{\max}$ and Θ.

3.2. Triangle networks and hexagon networks

Other regular topologies of interest are the triangle topology and its dual, the hexagon topology (Figure 5). For each triangle, there are three vertices and six nearest neighbors for each vertex, while for the hexagon, there are six vertices for each hexagon and three nearest neighbors for each vertex. Again, the next-hop receiver of each packet is one

[6] In fact, $\alpha \to 2$ is sufficient for infinite networks.

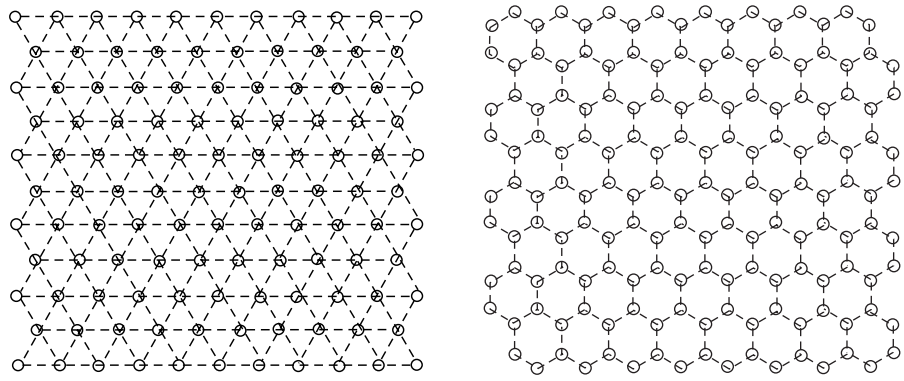

(a) (b)

Figure 5: The topology of (a) triangle network and (b) hexagon network.

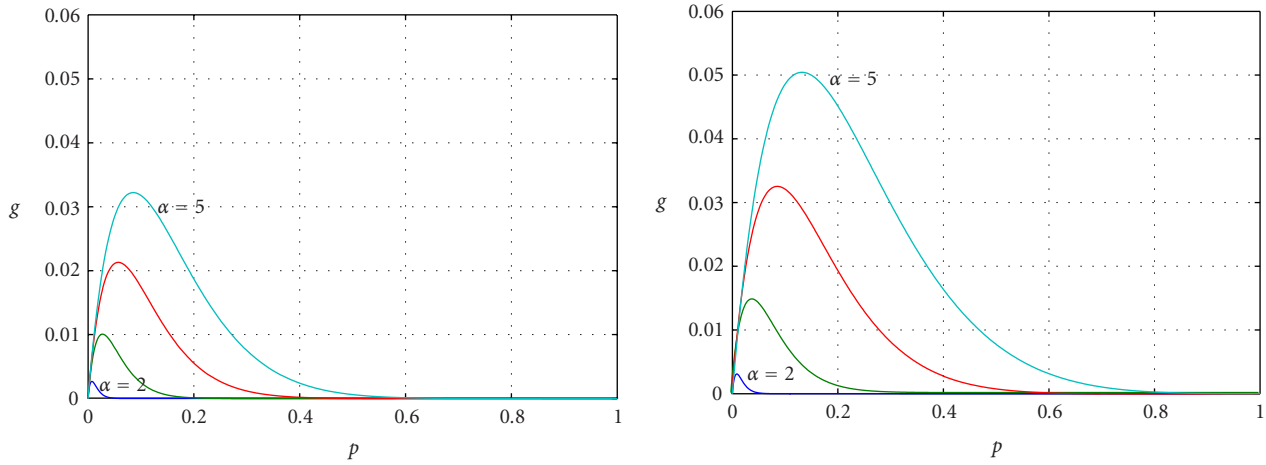

(a) (b)

Figure 6: The analytic throughput $g(p)$ versus p for two-dimensional networks with (a) triangle topology and (b) hexagon topology, where $\Theta = 10$ and $N = 1600$ nodes.

of the nearest-neighbor nodes of the transmitter, so the transmitter-receiver distance d_0 is equal to the side length of the regular polygon. In the triangle network, each node is located in a hexagon with area $(\sqrt{3}d_0^2)/2$. For node density equal to 1, $d_0^2 = 2/\sqrt{3}$. Similarly, for hexagon networks, $d_0^2 = 4/(3\sqrt{3})$.

Similar to the calculation of square lattice networks as in (7), we obtain the relationship between the throughput g and the transmit probability p and compare the performance of triangle and hexagon networks in Figure 6. For a fair comparison, we introduce the *transport capacity* which can be defined as $Z := g_{\max} d_0$. The results for square, triangle, and hexagon networks for $\alpha = 4$ are shown in Table 2. The performance difference among the three topologies can be explained by the distance and number of the potential interfering nodes. Note that the transmit efficiency T_{eff} is very close to the one of conventional slotted ALOHA and does not depend on the topology.

4. RANDOM NETWORKS

Here, we assume that the positions of the nodes constitute a Poisson point process.[7] In the following, we will investigate the throughput averaged over network realizations when the transmitter-receiver distance d_0 is fixed (Section 4.1) and not fixed (Section 4.2).

4.1. *Average throughput for fixed* d_0

In this case, we assume the distance between the desired transmitter and receiver is fixed and there are N other nodes constituting a two-dimensional Poisson point process. Although (6) gives the success probability conditioned on node distances, we still need to find the joint density of

[7] For large networks, this is equivalent to a uniformly random distribution for all practical purposes.

Table 2: Comparison of square, triangle, and hexagon networks for $\alpha = 4$ and $\Theta = 10$, where p_{opt}, $g_{\max}$, and T_{eff} denote the optimum transmit probability, maximum throughput, and transmit efficiency.

	p_{opt}	$g_{\max}$	T_{eff}	d_0	$g_{\max}d_0$
Square	0.0660	0.0247	0.37	1.0	0.0247
Triangle	0.0570	0.0213	0.37	1.0746	0.0229
Hexagon	0.0870	0.0326	0.37	0.8774	0.0286

$d_1, d_2, \ldots, d_N$ (ordered distances). It is well known that for one-dimensional Poisson point processes with density λ, the ordered distance from nodes to the desired receiver form the arrival times of a Poisson process [24]. The interarrival intervals are i.i.d. exponential with parameter λ:

$$f_{d_i - d_{i-1}}(x_i - x_{i-1}) = \lambda e^{-\lambda(x_i - x_{i-1})}. \tag{18}$$

So, for the ordered distance $0 \le d_1 \le \cdots \le d_N$, the joint density function of the interarrival intervals is

$$\begin{aligned} &f_{d_1,d_2,\ldots,d_N}(x_1, x_2, \ldots, x_N) \\ &\quad = f_{d_1,\ldots,d_N - d_{N-1}}(x_1, x_2 - x_1, \ldots, x_N - x_{N-1}) \\ &\quad = (\lambda e^{-\lambda x_1})(\lambda e^{-\lambda(x_2 - x_1)}) \cdots (\lambda e^{-\lambda(x_N - x_{N-1})}) \\ &\quad = \lambda^N e^{-\lambda x_N}, \quad 0 \le x_1 \le x_2 \le \cdots \le x_N. \end{aligned} \tag{19}$$

When nodes are distributed according to a two-dimensional Poisson point process with density λ, the squared ordered distances from the desired receiver have the same distribution as the arrival times of a Poisson process with density $\lambda\pi$ [24]. The squared ordered distances have a joint distribution with density

$$\begin{aligned} f_{d_1^2,\ldots,d_N^2}(x_1, \ldots, x_N) &= (\lambda\pi)^N e^{-\lambda\pi x_N}, \\ 0 \le x_1 \le x_2 \le \cdots \le x_N, & \end{aligned} \tag{20}$$

because from [26], we have

$$f_{d_i^2 - d_{i-1}^2}(x_i - x_{i-1}) = \lambda\pi e^{-\lambda\pi(x_i - x_{i-1})}. \tag{21}$$

The conditional success probability can be written as (see (6))

$$P_{s|d_0,d_1,\ldots,d_N} = \prod_{i=1}^{N} \frac{(d_i^2)^{\alpha/2} + (1-p)\Theta d_0^\alpha}{(d_i^2)^{\alpha/2} + \Theta d_0^\alpha}. \tag{22}$$

Integrating (22) with respect to the joint density (20), and in particular, evaluating it for $\alpha = 4$, we obtain

$$\begin{aligned} &P_{s|d_0} \\ &= \int_0^\infty (\lambda\pi)^N e^{-\lambda\pi x_N} \\ &\qquad \times \left\{ \int_0^{x_N} \cdots \int_0^{x_2} \prod_{i=1}^{N} \frac{x_i^2 + (1-p)\Theta d_0^4}{x_i^2 + \Theta d_0^4} dx_1 \cdots dx_{N-1} \right\} dx_N. \end{aligned} \tag{23}$$

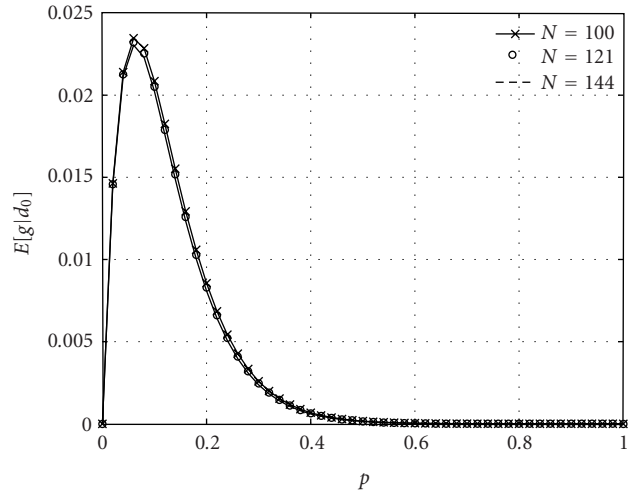

Figure 7: For $\alpha = 4$ and $\Theta = 10$, the analytical average throughput $\mathbb{E}[g|d_0 = 1]$ based on (25) for networks with node number $N = 100$, 121, and 144.

By applying a similar inductive technique as in [24], it can be shown that

$$\begin{aligned} &\int_0^{x_N} \cdots \int_0^{x_2} \prod_{i=1}^{N-1} \frac{x_i^2 + (1-p)\Theta d_0^4}{x_i^2 + \Theta d_0^4} dx_1 \cdots dx_{N-1} \\ &\quad = \frac{1}{(N-1)!} \left(x_N - p\sqrt{\Theta d_0^4} \arctan\left(\frac{x_N}{\sqrt{\Theta d_0^4}} \right) \right)^{N-1}. \end{aligned} \tag{24}$$

Combining (23) and (24), we have

$$\begin{aligned} P_{s|d_0} = \int_0^\infty &\frac{(\lambda\pi)^N}{(N-1)!} e^{-\lambda\pi x} \frac{x^2 + (1-p)\Theta d_0^4}{x^2 + \Theta d_0^4} \\ &\times \left(x - p\sqrt{\Theta d_0^4} \arctan\left(\frac{x}{\sqrt{\Theta d_0^4}} \right) \right)^{N-1} dx. \end{aligned} \tag{25}$$

Based on (25), we numerically evaluate the average throughput $\mathbb{E}[g|d_0] = p(1-p)P_{s|d_0}$ (averaged over all network realizations) and plot it as a function of p in Figure 7 for a network with node numbers $N = 100$, 121, and 144, where $d_0 = 1$. It is shown that they are very close, indicating that only a portion of the nodes interfere at the receiver and nodes further away have little impact on the transmission.

4.2. Average throughput for variable d_0

In the previous analysis, we assumed that the transmitter-receiver distance d_0 is fixed and there are N potential interfering nodes uniformly distributed. Now we assume that the receiver located at the center selects its nearest-neighbor node as its desired transmitter. Then there are $N - 1$ nodes further away than the desired transmitter. The distance to the nearest neighbor has the Rayleigh density function (as shown in [23])

$$f_{d_0}(x) = 2\pi x e^{-\pi x^2}. \tag{26}$$

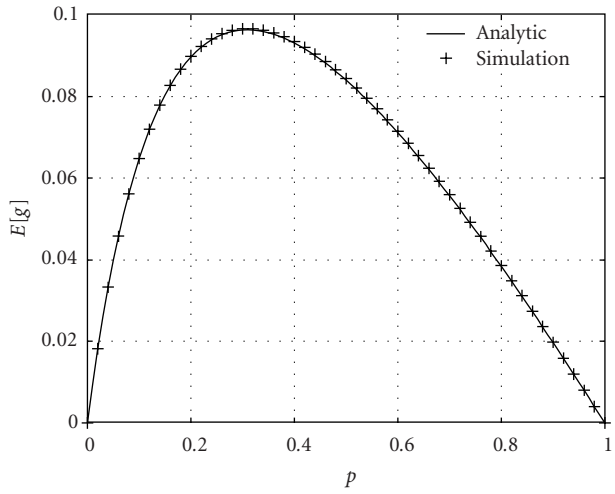

Figure 8: For $\alpha = 4$ and $\Theta = 10$, $\mathbb{E}[g]$ versus p for random network with $N = 144$. The analytic result from (27) and (30) is displayed by solid line; the simulation result over 10 000 runs by + mark.

Since d_0 is the nearest distance, d_i^2 in (22) can be varying from d_0^2 to d_{i+1}^2. So we integrate x_i from d_0^2 to x_{i+1}:

$$P_{s|d_0} = \int_{d_0^2}^{\infty} f_{d_1^2,\ldots,d_{N-1}^2|d_0^2}(x_1,\ldots,x_{N-1}|d_0^2) \times \left\{ \int_{d_0^2}^{x_{N-1}} \cdots \int_{d_0^2}^{x_2} \prod_{i=1}^{N-1} \frac{x_i^2+(1-p)\Theta d_0^4}{x_i^2+\Theta d_0^4} dx_1 \cdots dx_{N-2} \right\} dx_{N-1}, \quad (27)$$

$$f_{d_1^2,\ldots,d_{N-1}^2|d_0^2}(x_1,\ldots,x_{N-1}|d_0^2) = (\lambda\pi)^{N-1} e^{-\lambda\pi(x_{N-1}-d_0^2)}, \quad (28)$$

where $0 \le d_0^2 \le x_1 \le \cdots \le x_{N-1}$.

By induction, it can be shown that

$$\int_{d_0^2}^{x_{N-1}} \cdots \int_{d_0^2}^{x_2} \prod_{i=1}^{N-2} \frac{x_i^2+(1-p)\Theta d_0^4}{x_i^2+\Theta d_0^4} dx_1 \cdots dx_{N-2} = \frac{1}{(N-2)!} \left\{ x_{N-1} - d_0^2 - p\sqrt{\Theta d_0^4} \cdot \left[\arctan\left(\frac{x_{N-1}}{\sqrt{\Theta d_0^4}}\right) - \arctan\left(\frac{d_0^2}{\sqrt{\Theta d_0^4}}\right) \right] \right\}^{N-2}. \quad (29)$$

The success probability is $P_{s|d_0}$ averaged over d_0:

$$P_s = \int_0^{\infty} f_{d_0}(x) P_{s|d_0} dx. \quad (30)$$

Substitute (28) and (29) into (27) and evaluate (30) with (26), we obtain the relationship between $\mathbb{E}[g] = p(1-p)P_s$ and p, which is plotted in Figure 8. It is shown that the analytic (solid line) and simulation result (marked by +) match perfectly.

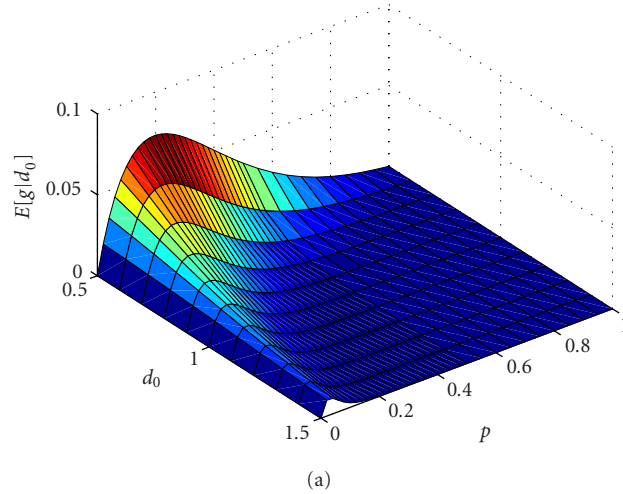

(a)

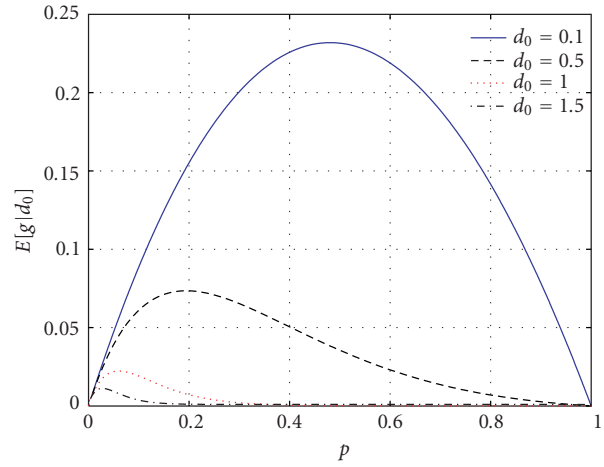

(b)

Figure 9: For $\alpha = 4$ and $\Theta = 10$, average throughput (a) $\mathbb{E}[g|d_0]$ versus p for d_0 from 0.5 to 1.5; (b) $\mathbb{E}[g|d_0]$ versus p for $d_0 = 0.1$, 0.5, 1.0, and 1.5.

Figure 8 implies random networks have better average throughput for local data exchange than regular networks. This can be explained by d_0, the transmitter-receiver distance. In random networks, a variable d_0 leads to a variable throughput. Figure 9a displays $\mathbb{E}[g|d_0]$ versus p for d_0 from 0.5 to 1.5. Figure 9b shows the relationship for $d_0 = 0.1, 0.5, 1.0$, and 1.5. Not surprisingly, smaller d_0 results in higher throughput. For the variable d_0 case, it is assumed that the desired transmitter is the nearest neighbor of the receiver. With the pdf of (26), the probability that d_0 is greater than 1 (the transmitter-receiver distance in the square lattice network) is $\mathbb{P}[d_0 > 1] = e^{-\pi} = 0.043$. So for most nodes, the received signal power from the desired transmitter is greater than that in regular networks. In Figure 9b, for $d_0 = 0.1$, it is shown that the strong signal power resulting from very small d_0 offsets the impact of interference even for high transmit probabilities p.

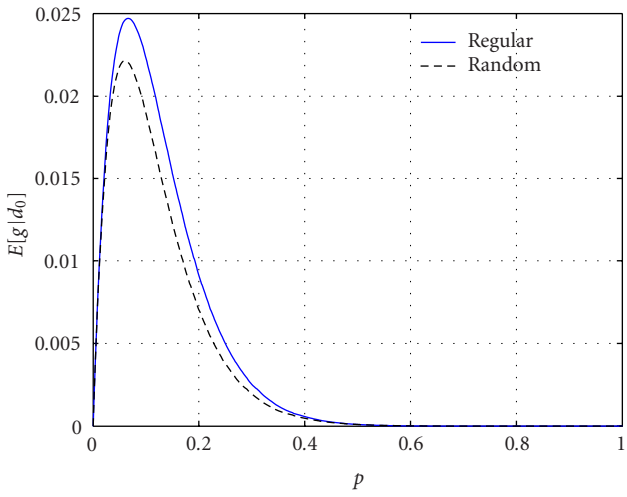

FIGURE 10: Comparison of the average throughput of regular square network and random network. For both networks, $N = 1600$, $d_0 = 1$, $\alpha = 4$, and $\Theta = 10$.

Now consider the generic routing strategy from [23]: each node in the path sends packets to its nearest neighbor that lies within a sector ϕ, that is, within $\pm\phi/2$ of the source-destination direction. The previous scheme where d_0 is obtained as the distance to the nearest neighbor makes no progress in the source-destination direction. Such a choice of d_0 would correspond to routing within $\phi = 2\pi$, clearly an inefficient choice of ϕ. More sensible is $\phi \leq \pi$. Let d_0 be the distance to the nearest neighbor within sector ϕ. The probability density of d_0 is given by [23]

$$f_{d_0}(x) = x\phi e^{-x^2\phi/2}. \tag{31}$$

If the routing sector $\phi = \pi/2$, then $\mathbb{E}[d_0] = 1$. For $d_0 = 1$, Figure 10 displays the throughput for square network and random network with $N = 1600$. It turns out that for the same transmitter-receiver distance, square networks have a slightly higher average throughput than random networks.

We compare the transport capacity $g_{\max} d_0$ of regular and random networks. Figure 11a shows $g_{\max}$ versus d_0 and p_{opt} versus d_0 for a random network. Figure 11b compares the transport capacity of random and regular networks. It is shown that at a specific transmitter-receiver distance d_0, regular networks slightly outperform random networks in terms of transport capacity.

4.3. End-to-end throughput g_{EE} in a random network

In wireless sensor networks with multihop communication, the end-to-end throughput (the minimum of the throughput values of the links involved) of a route with an average number of hops is a better performance indicator than the average throughput. For two-dimensional random sensor networks (busy area $m \times m$, density 1, routing within sector ϕ) with uniformly randomly selected source and fixed destination located at the corner,[8] we can approximate the average path length in hops

$$\bar{h} \approx \frac{\bar{r}}{\bar{D}\eta}, \tag{32}$$

where $\bar{r}$ denotes the expected distance between the source and the destination, $\bar{D}$ the expected hop length, and η the expected path efficiency, where the path efficiency is the ratio between the Euclidean distance and the travelled distance of a path. $\bar{D}\eta$ can be viewed as the effective hop length—the average hop length projected onto the source-destination axis. The expected distance from a random point in a square to a corner can be derived from [27, Exercise 2.4.5]:

$$\bar{r} = \left[\frac{\sqrt{2}}{3} + \frac{1}{3}\operatorname{arctanh}\left(\frac{1}{\sqrt{2}}\right)\right] m \approx 0.769m. \tag{33}$$

From [23], we know that

$$\bar{D} = \sqrt{\frac{\pi}{2\phi}}, \qquad \eta = \frac{2}{\phi}\sin\left(\frac{\phi}{2}\right). \tag{34}$$

So the average path length in hops can be approximated by plugging (33) into (32). To evaluate the end-to-end throughput of a route with $\bar{h}$ hops, we use a semianalytic approach by generating an $\bar{h}$-hop path with each hop length obtained as a realization of D according to the pdf in (31), and evaluate the throughput of each hop based on Figure 9a. The average end-to-end throughput is then obtained by taking the minimum of each path and averaging the minimum over the number of realizations of the simulated routes. It is shown in Figure 12 that the maximum end-to-end throughput g_{EE} is 0.0086, 0.0053, and 0.0039 for $\phi = \pi$, $\pi/2$, and $\pi/3$.

What is the end-to-end throughput for regular networks? It can be directly obtained from Figures 2 and 6, which is 0.0247, 0.0213, and 0.0326 for square, triangle, and hexagon networks. For regular networks, every hop has the same length, and the throughput is calculated for a link in the center of the network, which is the worst case, so the end-to-end throughput is the throughput of the center link of the busy area. In terms of the end-to-end throughput for multihop communication, regular networks significantly outperform random networks. For larger networks, the benefit is larger since larger m results in longer paths.

5. CONCLUSIONS

We have shown that for a noiseless Rayleigh fading network with slotted ALOHA, the success probability of a transmission is the Laplace transform of the interference evaluated at the SIR threshold Θ. We assume that in every timeslot, each

[8] For the many-to-one traffic typical in sensor networks, we assume the data sink for all connections to be in one of the corners of the (square) network.

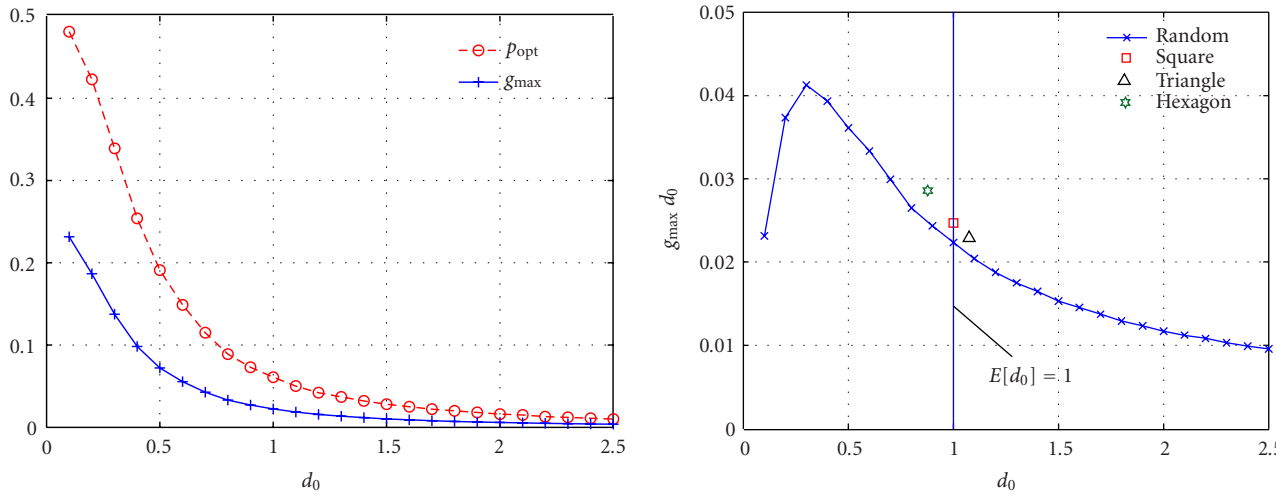

FIGURE 11: With $N = 1600$, $\alpha = 4$, and $\Theta = 10$, (a) g_{max} versus d_0 and p_{opt} versus d_0 for a random network; (b) transport capacity $g_{max}d_0$ for random and regular networks with the same size and node density. For random networks, $\mathbb{E}[d_0] = 1$ for $\phi = \pi/2$.

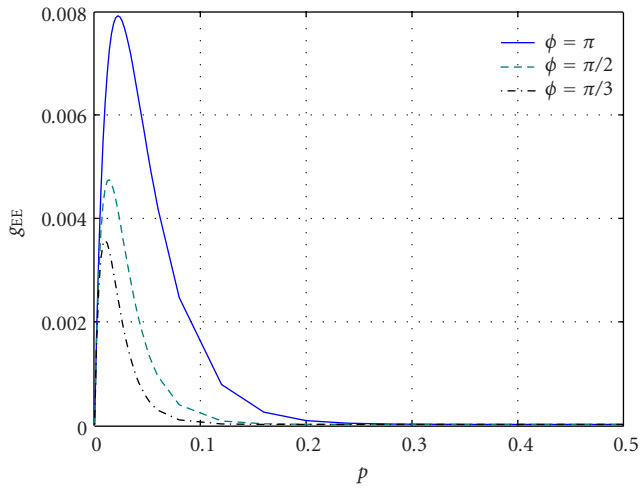

FIGURE 12: The average end-to-end throughput of random networks for different routing sectors ϕ, where $\alpha = 4$ and $\Theta = 10$.

node transmits independently with a certain fixed probability $p = p_q p_t$, where p_q is the intensity of the Bernoulli traffic and p_t is the channel access probability. This decomposition of p shows that the throughput analysis and optimization with respect to p includes a range of traffic intensities and channel access probabilities.

Among the three regular networks (square, triangle, hexagon), the hexagon network provides the highest throughput since every node has only three nearest neighbors which is the smallest among the three networks. The sensitivity analysis of the maximum throughput g_{max} and optimum transmit probability p_{opt} with respect to Θ for square networks explains why the transmit efficiency $T_{eff} = g_{max}/p_{opt}$ is approximately 37%. These results hold quantitatively for the other two regular networks—triangle and hexagon networks.

For random networks, two scenarios are considered—fixed and variable transmitter-receiver distances d_0. If d_0 is the same for regular and random networks, regular networks slightly outperform random networks in terms of throughput and transport capacity. In the case of variable d_0 where the receiver selects the nearest-neighbor node as its desired transmitter, the average throughput of random networks is better than that of regular ones. This is because strong signal powers resulting from very small d_0 offset the impact of interference even for high transmit probabilities. This result, however, only pertains to local data exchange. When multihop communication and routing is taken into account, regular topologies have a significant advantage in terms of end-to-end throughput. The reason for the inferior end-to-end performance of random networks is the large variance in the node distances.

ACKNOWLEDGMENT

The support of the US National Science Foundation (Grants ECS 03-29766 and CAREER CNS 04-47869) is gratefully acknowledged.

REFERENCES

[1] I. F. Akyildiz, W. Su, Y. Sankarasubramaniam, and E. Cayirci, "Wireless sensor networks: a survey," *Computer Networks*, vol. 38, no. 4, pp. 393–422, 2002.

[2] P. Gupta and P. R. Kumar, "The capacity of wireless networks," *IEEE Trans. Inform. Theory*, vol. 46, no. 2, pp. 388–404, 2000.

[3] S. Toumpis and A. J. Goldsmith, "Capacity regions for wireless ad hoc networks," *IEEE Transactions on Wireless Communications*, vol. 2, no. 4, pp. 736–748, 2003.

[4] J. Silvester and L. Kleinrock, "On the capacity of multihop slotted ALOHA networks with regular structure," *IEEE Trans. Commun.*, vol. 31, no. 8, pp. 974–982, 1983.

[5] M. Grossglauser and D. Tse, "Mobility increases the capacity

of ad hoc wireless networks," in *Proc. 20th Annual Joint Conference of the IEEE Computer and Communications Societies (INFOCOM '01)*, vol. 3, pp. 1360–1369, Anchorage, Alaska, USA, April 2001.

[6] D. Marco, E. Duarte-Melo, M. Liu, and D. L. Neuhoff, "On the many-to-one transport capacity of a dense wireless sensor network and the compressibility of its data," in *Proc. 2nd IEEE International Workshop on Information Processing in Sensor Networks (IPSN '03)*, pp. 1–16, Palo Alto, Calif, USA, April 2003.

[7] L.-L. Xie and P. R. Kumar, "A network information theory for wireless communication: scaling laws and optimal operation," *IEEE Trans. Inform. Theory*, vol. 50, no. 5, pp. 748–767, 2004.

[8] S. De, C. Qiao, D. A. Pados, and M. Chatterjee, "Topological and MAI constraints on the performance of wireless CDMA sensor networks," in *Proc. 23rd Annual Joint Conference of the IEEE Computer and Communications Societies (INFOCOM '04)*, vol. 1, Hong Kong, China, March 2004.

[9] G. Ferrari and O. K. Tonguz, "Performance of ad hoc wireless networks with Aloha and PR-CSMA MAC protocol," in *Proc. IEEE Global Telecommunications Conference (GLOBECOM '03)*, vol. 5, pp. 2824–2829, San Francisco, Calif, USA, December 2003.

[10] S. Panichpapiboon, G. Ferrari, and O. K. Tonguz, "Sensor networks with random versus uniform topology: MAC and interference considerations," in *Proc. IEEE Vehicular Technology Conference (VTC '04)*, vol. 4, pp. 2111–2115, Milan, Italy, May 2004.

[11] E. S. Sousa and J. A. Silvester, "Optimum transmission ranges in a direct-sequence spread-spectrum multihop packet radio network," *IEEE J. Select. Areas Commun.*, vol. 8, no. 5, pp. 762–771, 1990.

[12] N. H. Shepherd, et al., "Coverage prediction for mobile radio systems operating in the 800/900 MHz frequency range," *IEEE Trans. Veh. Technol.*, vol. 37, no. 1, pp. 3–72, 1988, Special issue on radio propagation.

[13] A. J. Goldsmith and S. B. Wicker, "Design challenges for energy-constrained ad hoc wireless networks," *IEEE Wireless Communications*, vol. 9, no. 4, pp. 8–27, 2002.

[14] A. Ephremides, "Energy concerns in wireless networks," *IEEE Wireless Communications*, vol. 9, no. 4, pp. 48–59, 2002.

[15] A. Woo, T. Tong, and D. Culler, "Taming the underlying challenges of reliable multihop routing in sensor networks," in *Proc. 1st International Conference on Embedded Networked Sensor Systems*, pp. 14–27, Los Angeles, Calif, USA, November 2003.

[16] S. Megerian, F. Koushanfar, G. Qu, G. Veltri, and M. Potkonjak, "Exposure in wireless sensor networks: theory and practical solutions," *Wireless Networks*, vol. 8, no. 5, pp. 443–454, 2002.

[17] N. Abramson, "The aloha system - another alternative for computer communications," in *Proc. Fall Joint Computer Conference, AFIPS Conference*, vol. 37, pp. 281–285, Houston, Tex, USA, November 1970.

[18] F. Tobagi, "Analysis of a two-hop centralized packet radio network—Part I: slotted ALOHA," *IEEE Trans. Commun.*, vol. 28, no. 2, pp. 196–207, 1980.

[19] F. Baccelli, B. Blaszczyszyn, and P. Mühlethaler, "A Spatial Reuse Aloha MAC Protocol For Multihop Wireless Mobile Networks," Tech. Rep. 4955, Institut National de Recherche en Informatique et en Automatique (INRIA), Rocquencourt, Le Chesnay Cedex, France, October, 2003, Available at http://www.terminodes.org/MV2003-Present/Me15/Spacial-Baccelli.pdf.

[20] R. Nelson and L. Kleinrock, "The spatial capacity of a slotted ALOHA multihop packet radio network with capture," *IEEE Trans. Commun.*, vol. 32, no. 6, pp. 684–694, 1984.

[21] D. Bertsekas and R. Gallager, *Data Networks*, Prentice-Hall, Englewood Cliffs, NJ, USA, 2nd edition, 1991.

[22] M. Haenggi, "Energy-balancing strategies for wireless sensor networks," in *Proc. IEEE International Symposium on Circuits and Systems (ISCAS '03)*, vol. 4, pp. IV-828–IV-831, Bangkok, Thailand, May 2003.

[23] M. Haenggi, "On routing in random Rayleigh fading networks," to appear in *IEEE Transactions on Wireless Communications*, http://www.nd.edu/~mhaenggi/.

[24] R. Mathar and J. Mattfeldt, "On the distribution of cumulated interference power in Rayleigh fading channels," *Wireless Networks*, vol. 1, no. 1, pp. 31–36, 1995.

[25] N. Ahmed and R. G. Baraniuk, "Throughput measures for delay-constrained communications in fading channels," in *Proc. Allerton Conference on Communication, Control and Computing*, Monticello, Ill, USA, October 2003.

[26] M. Hellebrandt and R. Mathar, "Cumulated interference power and bit-error-rates in mobile packet radio," *Wireless Networks*, vol. 3, no. 3, pp. 169–172, 1997.

[27] A. M. Mathai, *An Introduction to Geometrical Probability*, Gordon and Breach Science Publishers, New York, NY, USA, 1999.

Xiaowen Liu received the M.S. degree in signal and information processing from the Institute of Acoustics, Chinese Academy of Sciences, in 1998. She entered the University of Notre Dame as a graduate student in January 2001. She earned the Master degree in electrical engineering in 2002. Currently, she is working toward the Ph.D. degree in the Department of Electrical Engineering. Her current research interests include wireless network and communications, especially the performance analysis of wireless ad hoc and sensor networks.

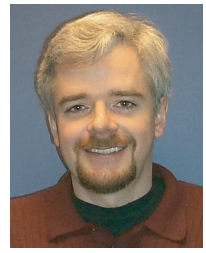

Martin Haenggi received the Dipl. Ing. (M.S.) degree in electrical engineering from the Swiss Federal Institute of Technology in Zurich (ETHZ) in 1995. In 1995, he joined the Signal and Information Processing Laboratory at ETHZ as a Teaching and Research Assistant. In 1996, he earned the Dipl. NDS ETH (post-diploma) degree in information technology, and in 1999, he completed his Ph.D. thesis on the analysis, design, and optimization of cellular neural networks. After a postdoctoral year at the Electronics Research Laboratory, the University of California in Berkeley, he joined the faculty of the Electrical Engineering Department, the University of Notre Dame, as an Assistant Professor in January 2001. For both his M.S. and his Ph.D. theses, he was awarded the ETH Medal, and he received a CAREER Award from the US National Science Foundation in 2005. He is a Member of the Editorial Board of the Elsevier Journal on Ad Hoc Networks. His scientific interests include networking and wireless communications, with an emphasis on ad hoc and sensor networks.